Urea-Chelation of I^+ for High Voltage Aqueous Zinc-Iodine Batteries

Cuicui Li[1], Haocheng Li[6], Xiuyun Ren[2], Liang Hu[2], Jiaojiao Deng[4], Jinhan Mo, Xiaoqi Sun[3,], Guohua Chen[1,*], Xiaoliang Yu[2,*]*

[1] School of Energy and Environment, City University of Hong Kong, Hong Kong 999077, China

[2] Department of Mechanical Engineering and Research Institute for Smart Energy, The Hong Kong Polytechnic University, Hong Kong 999077, China

[3] Department of Chemistry, Northeastern University, 3-11 Wenhua Road, Shenyang 110819, China

[4] Graphene Composite Research Center, College of Chemistry and Environmental Engineering, Shenzhen University, Shenzhen 518060, China

[5] College of Civil and Transportation Engineering, Shenzhen University, Shenzhen 518060, China

[6] School of Mechanical Engineering, Beijing Institute of Technology, Beijing 100081, China

KEYWORDS: zinc-iodine battery, multi-electron conversion, urea chelation, high voltage, high stability

ABSTRACT

The multi-electron conversion electrochemistry of $I^-/I^0/I^+$ enables high specific capacity and voltage in zinc-iodine batteries. Unfortunately, the I^+ ions exhibit thermodynamic instability and a high susceptibility to hydrolysis. Current endeavors primarily focus on exploiting interhalogen chemistry to activate the I^0/I^+ couple, which, however, corrodes the battery components, and the working voltage is below the theoretical level. In this study, the I^0/I^+ redox couple is fully activated, and I^+ is efficiently stabilized by a chelation agent of cost-inexpensive urea in the conventional aqueous electrolyte. A record-high plateau voltage of 1.8 V vs. Zn/Zn^{2+} has been realized. Theoretical calculations combining spectroscopy studies and electrochemical tests reveal that the coordination between the electron-deficient I^+ and electron-rich O and N atoms in urea molecules is more thermodynamically favorable for I^0/I^+ conversion and inhibits the self-disproportionation of I^+, which promotes rapid kinetics and excellent reversibility. Moreover, urea reduces the water activity in the electrolyte by forming hydrogen bonds to further suppress the hydrolysis of I^+. Accordingly, a high specific capacity of 419 mAh g^{-1} is delivered at 1C, and 147 mAh g^{-1} capacity was maintained after 10000 cycles at 5C. This work offers new insights into formulating halogen-free electrolytes for high-performance aqueous zinc-iodine batteries.

INTRODUCTION

Rechargeable aqueous zinc batteries (RAZBs) hold great promise for grid-scale energy storage due to their intrinsic safety, greenness, and low production cost.[1-3] However, the energy density of RAZBs is limited by the low working voltage and specific capacity of cathode materials.[4,5] In the past decade, significant efforts have been devoted to exploiting high-voltage and high-capacity cathodes, such as V/Mn-based transition metal compounds,[6-8] electrochemically active organics,[9-11] and conversion-type cathodes (I_2, Br_2, S).[12,13] Among them, the iodine cathode has attracted significant attention because of its high specific capacity and rapid conversion kinetics.[14,15] Currently reported aqueous zinc-iodine batteries are primarily based on the reversible I−/I0 conversion, which delivers an output plateau voltage below 1.3 V vs. Zn/Zn2+ and a theoretical capacity of 211 mAh g^{-1}.[16] In fact, iodine exhibits multiple valance states, which allows fascinating multi-electron conversion reactions.[17] Recently, the four-electron conversion electrochemistry of $2I^-/I_2/2I^+$ has been developed in Zn-I_2 batteries, doubling the theoretical capacity to as high as 422 mAh g^{-1} and generating an additional high plateau voltage of 1.8 V vs. Zn/Zn^{2+}.[18,19] Despite their attractiveness, the I^+ ions experience thermodynamic instability and a high susceptibility to hydrolysis in aqueous electrolytes.[20,21] It results in a significant challenge in activating the I^0/I^+ redox couple and improving the conversion reaction reversibility.

The solution to this critical issue depends on formulating proper electrolytes to suppress I^+ decomposition and facilitate reversible I^0/I^+ conversion.[22] Recent endeavors primarily focus on exploiting interhalogen chemistry between iodine in the cathode and halide in the electrolyte to stabilize I^+.[18, 19, 23-25] As a typical example, Liang et al. reported a highly concentrated electrolyte of 19 m LiCl, 19 m $ZnCl_2$, and 8 m acetonitrile in water to inhibit I^+ hydrolysis while providing abundant free Cl^- to promote I^0/I^+ conversion reaction.[19] He et al. introduced tetraethylammonium

cations to the 15 m $ZnCl_2$ electrolyte as ion sieves, which can dynamically modulate the electrode-electrolyte interface and inhibit the ICl hydrolysis.[26] However, the Zn anode and battery components are susceptible to corrosion by the Cl^- containing electrolyte. Given that the electrophilic I^+ could bond with nucleophilic species to form charge-transfer complexes.[27] Liu et al. conducted a pioneering work very recently in which a halogen-free eutectic electrolyte helps stabilize I^+ through robust coordination with niacinamide.[28] Nevertheless, the important advantages of low cost for aqueous batteries would be affected by applying high salt concentration or eutectic electrolytes. Besides, we note that the I^0/I^+ redox potentials in these reported studies are around 1.65 V vs. Zn/Zn^{2+}, below the theoretical value of 1.8 V vs. Zn/Zn^{2+}. Therefore, developing cost-effective halogen-free electrolytes to anchor I^+ and support high-voltage zinc-iodine batteries is still challenging.

Herein, we apply the cost-inexpensive urea as the additive in the zinc trifluoromethanesulfonate ($Zn(OTf)_2$) electrolyte to chelate with and stabilize I^+, therefore boosting the charge storage with $I^-/I^0/I^+$ reversible conversions in aqueous zinc-iodine batteries. Notably, the I^0/I^+ redox couple is fully activated and provides a record-high plateau voltage of 1.8 V vs. Zn/Zn^{2+}. Density functional theory (DFT) calculations and experimental analyses reveal that the chelation sites exist on the electron-rich O and N atoms of urea molecules. It is more thermodynamically favorable for I^0/I^+ conversion, which ensures facilitated reaction kinetics and excellent reversibility. Besides, the resulting I^+-ON (urea) complex presents a much larger energy gap between frontier orbitals. Therefore, the self-disproportionation reaction is inhibited. The reduced water activity in the electrolyte by forming hydrogen bonds with urea further prevents the hydrolysis of I^+. Accordingly, a high specific capacity of 419 mAh g^{-1} is delivered at 1C, and 147 mAh g^{-1} capacity was maintained after prolonged 10000 cycles at 5C. This work offers new

insights into formulating halogen-free electrolytes for high-voltage and stable aqueous zinc-iodine batteries.

RESULTS AND DISCUSSION

In this study, polyvinylpyrrolidone-iodine (PVPI) was employed as an electrochemically stable iodine-containing cathode in RAZBs for investigation, in which iodine species are bonded with the PVP substrate via robust chemical interaction.[29] Their electrochemical properties were studied in $Zn(OTf)_2$ and zinc chloride ($ZnCl_2$)-based aqueous electrolytes as well as a urea-added $Zn(OTf)_2$ electrolyte (designated as $Zn(OTf)_2$, $ZnCl_2$, and $Zn(OTf)_2$/urea, respectively, **Figure 1**a,b. In the $Zn(OTf)_2$ electrolyte, the only low-voltage plateau corresponds to the I^-/I^0 conversion reaction. No high-voltage plateau corresponding to the I^+/I^0 conversion can be observed due to the quick hydrolysis of I^+ under high potentials.[30] When $Zn(OTf)_2$ was replaced by $ZnCl_2$, the formation of the ICl intermediate in the $ZnCl_2$ electrolyte stabilizes I^+ and leads to a high voltage plateau at 1.6 V vs. Zn/Zn^{2+}, which, however, is far below the theoretical value of 1.83 V.[31] In contrast, after urea was added to the $Zn(OTf)_2$ electrolyte, a record-high discharge voltage plateau slightly over 1.8 V vs. Zn/Zn^{2+} presents. **Figure 1**c compares such a high plateau voltage to those of previous studies with I^0/I^+ conversion, showing the superiority of our system.[18,19,24,25,28,32-34] More impressively, such plateau voltage only declines marginally as the discharge rate increases from 1C to 5C (Figure 1d, C-rate defined based on 422 mAh giodine^{-1}), indicating the rapid kinetics of I^0/I^+ conversion. Rate performance shows highly reversible capacities of 419, 382, 342, 310, and 285 mA h g^{-1} at various rates of 1C, 2C, 3C, 4C, and 5C, respectively (**Figure S1**). The cycling stability of the PVPI cathode in the $Zn(OTf)_2$/urea electrolyte was demonstrated in **Figure 1**e. After prolonged 10000 cycles at 5C, the cathode maintains 147 mAh g^{-1} capacity. Such excellent

long-term cyclic stability can be ascribed to the stabilized I^+ and reduced activity of H_2O molecules in the aqueous electrolyte, which will be discussed in detail.

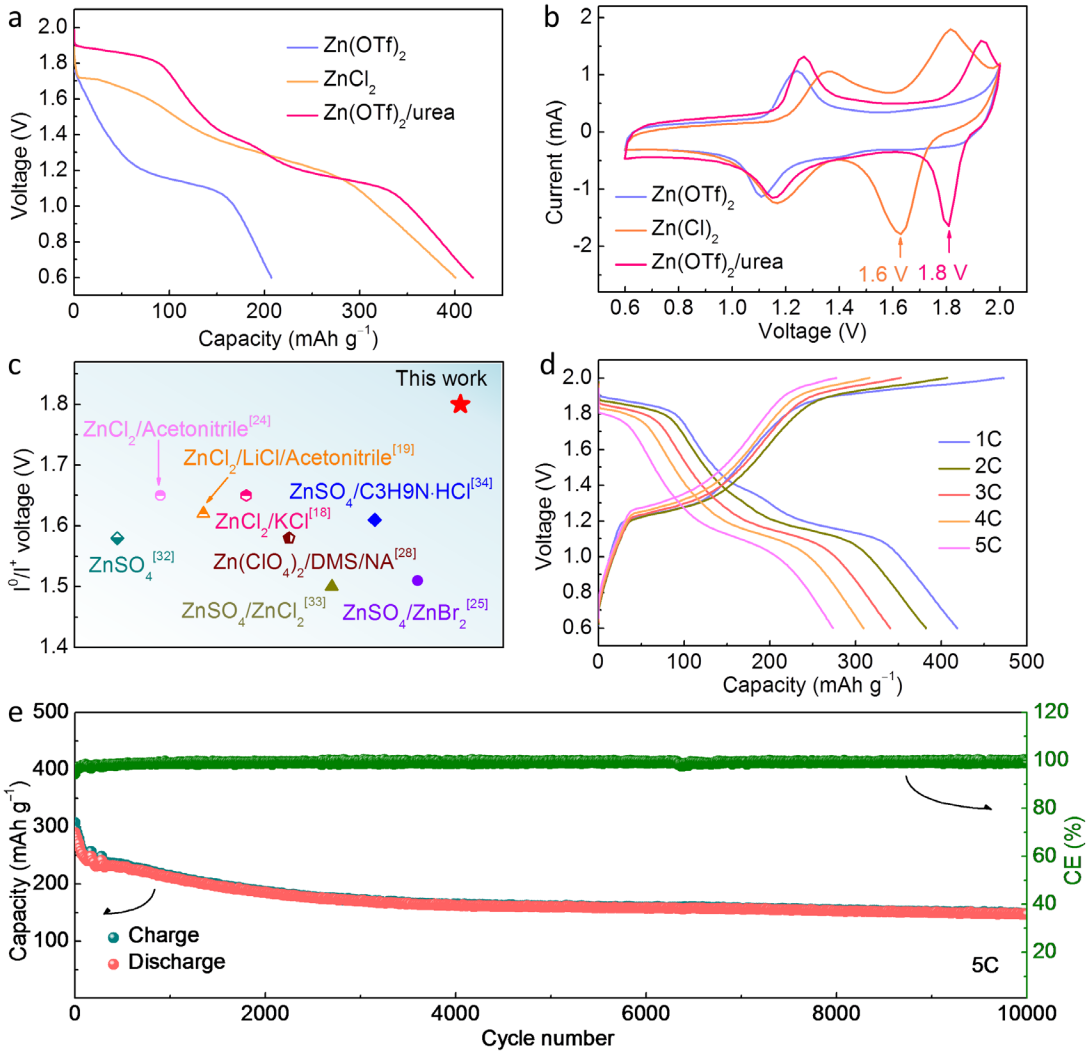

Figure 1. a) The discharge curves and b) cyclic voltammetry (CV) curves of the PVPI cathode in different electrolytes at the current density of 1C. c) Comparison of the high plateau voltage of this work to the reported aqueous zinc-iodine batteries. d) Charge/discharge curves of the PVPI cathode at various current rates. e) Long-term cycling stability of the PVPI cathode at 5C for 10000 cycles.

The effect of urea additive in modulating the electrochemical performance of iodine is studied. The urea molecule exhibits multiple electron-rich sites of N and O to coordinate with the electron-deficient I^+. DFT theoretical simulations reveal two feasible coordination modes, i.e., I^+ interactions with O + N or with two N sites as illustrated in **Figure 2**a (designated as I^+-ON (urea) and I^+-NN (urea), respectively). Notably, the former presents a much stronger binding energy (Eb) of −3.18 eV than −1.42 eV for the latter. The molecular electrostatic potential (MEP) distributions of urea and I^+-urea complexes were simulated. As shown in Figure 2b, the urea molecular displays more negative charges around the C=O bond than the amino sites, which explains the stronger binding energies with I^+ by the ON site than NN. Besides, the I^+-ON (urea) structure possesses a more uniform electron cloud distribution compared with I^+-NN (urea) (**Figure 2**c,d), suggesting the higher stability of the former.[35] It would help to stabilize I^+ and suppress its hydrolysis. To further reveal the structure requirements, the binding energies of I^+ with two other molecules of acetamide and acetone were calculated. The binding energy of I^+-ON (acetamide) was calculated to be −3.16 eV, which is very similar to −3.18 eV of I^+-ON (urea). The acetone molecule with only one carbonyl binding site, on the other hand, presents a weaker binding energy of −2.85 eV. The CV tests in the $Zn(OTf)_2$ electrolytes containing acetamide or acetone additive were further performed. As shown in **Figure 2**e, no characteristic peak corresponding to the I^0/I^+ conversion can be detected in the acetone-containing electrolyte, whereas the high-voltage peak appears in the acetamide-containing electrolyte. The results anticipated that the robust I^+-ON chelation is critical in stabilizing I^+ and activating the I^0/I^+ conversion.

To study the reaction activities of I^+ species, the frontier molecular orbital energy levels of I^+ and two I^+-urea complexes were evaluated by DFT. The lowest unoccupied molecular orbital (LUMO) and highest occupied molecular orbital (HOMO) energy levels are provided in Figure 2f.

Notably, I^+-ON (urea) shows a much wider energy gap (3.72 eV) than I^+ (1.19 eV) and I^+-NN (urea) (1.49 eV), suggesting its higher resistivity against self-disproportionation.[23] The Gibbs free energies of I^-, I_2, I^+, and different I^+-species are further calculated and shown in **Figure 2**g. The Gibbs free energy change (ΔG) from I^- to I_2 and I_2 to I^+ are determined to be 10.1 eV and 14.9 eV, respectively. Notably, this ΔG for I_2/I^+ conversion is much higher than that for I_2/I^+-urea complexes, which presents the value of 5.5 eV for I_2/I^+-ON (urea) and 7.2 eV for I_2/I^+-NN (urea). It suggests much more thermodynamically favorable for the I^0/I^+ reaction after coordinating I^+ to urea, and the chelation by the O and N sites presents the highest effectiveness. The interaction behavior in the I^+-ON (urea) complex is further calculated. As shown in the differential charge density, charge transfer occurs between −ON− sites in urea and I^+ (**Figure 2**h), ensuring a strong bond.[34] **Figure 2**i presents the atomic charges of I, O, and N in I^+-ON (urea). Opposite charge states are found on I vs. O and N centers in I^+-ON (urea), which favors robust interactions. The results confirm that urea promotes the generation I^+ and enhances its stability through chelation.

In addition to the interaction with active iodine species, urea also modulates the hydrogen bonding network in the electrolyte. In both Raman and Fourier transform infrared (FTIR) spectra, the characteristic bands from $–NH_2$ stretching vibrations of urea experience blue shifts in the $Zn(OTf)_2$/urea electrolyte (**Figure S2,3**),[36] implicating the formation of strong hydrogen bonds between urea and H_2O.[37,38] Nuclear magnetic resonance (NMR) measurements show that the peaks for 1H NMR of H_2O are shifted upfield in the $Zn(OTf)_2$/urea electrolyte as compared to the $Zn(OTf)_2$ electrolyte (**Figure S4**).[39] This suggests that the introduction of urea forms hydrogen bonds with H_2O molecules and disrupts the H_2O network, resulting in the upfield shift of ^1H NMR.[40,41] The generated urea-H_2O hydrogen bonds in the electrolyte reduce the amount of free

water molecules and their activity, thereby inhibiting the hydrolysis of I^+ and further ensuring its stability.

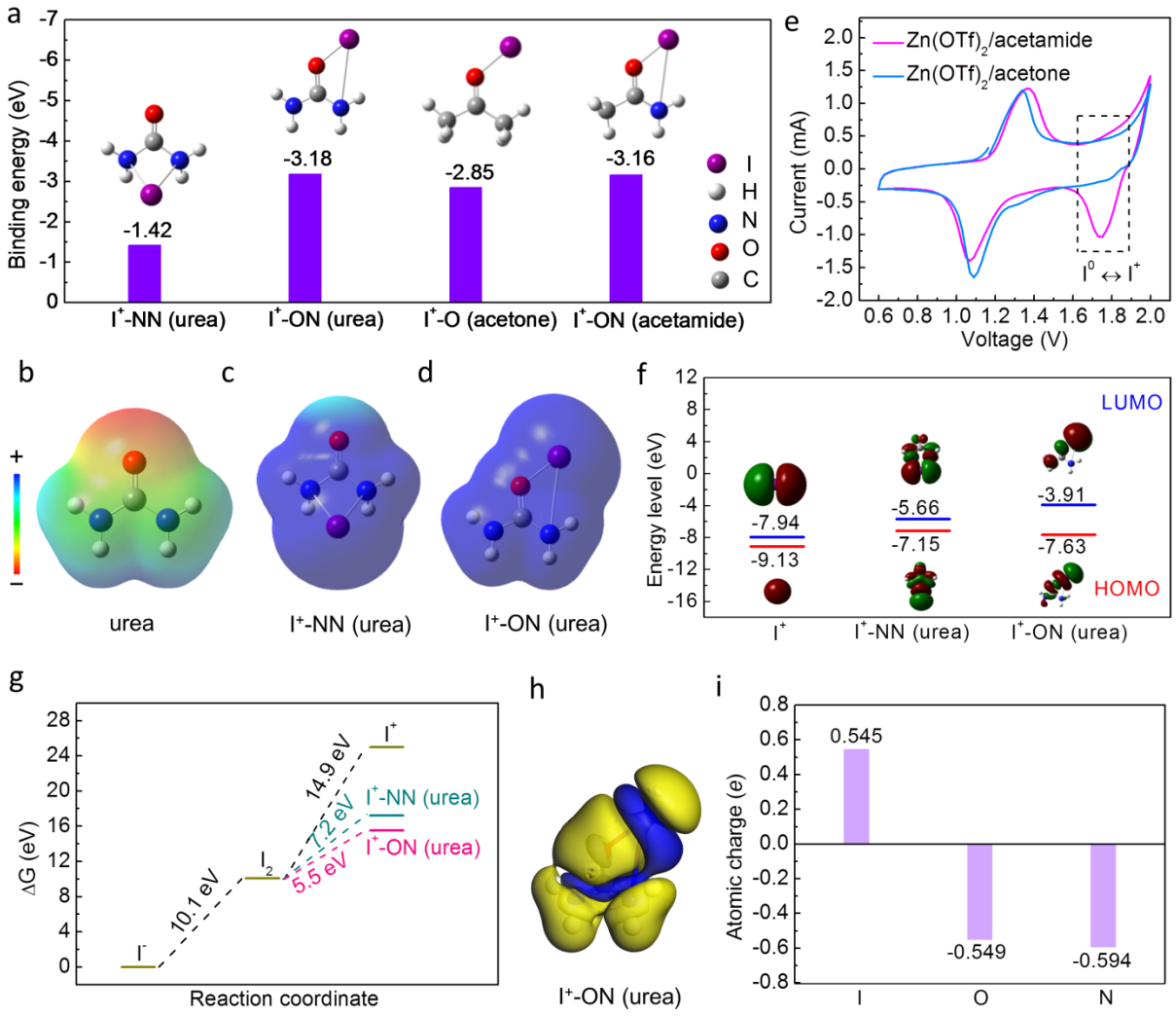

Figure 2. a) Binding energy, ESP of b) urea, c) I^+-NN (urea), and d) I^+-ON (urea). e) CV curves, and f) frontier molecular orbital energy levels of I^+ and different I^+ complexes. g) The calculated Gibbs free energies of I^-, I_2, I^+, and I^+-urea complexes. h) Differential charge density of I^+-ON (urea). i) The calculated atomic charges of I, O, and N in I^+-ON (urea).

To understand the iodine conversion reaction in the as-fabricated zinc-iodine batteries, X-ray photoelectron spectroscopy (XPS) was conducted to examine the valence transition during

charge/discharge (**Figure 3**a). The peaks at 617.8 eV and 629.3 eV in the pristine PVPI cathode correspond to the I $3d_{5/2}$ and I $3d_{3/2}$ splittings of I^- species, respectively. They shift to higher binding energies of 619.6 eV and 631.1 eV after full charge, suggesting the oxidation to a higher valence state of I^+. These peaks shift back to 618.2/629.8 eV upon full discharge to 0.6 V, demonstrating the reduction to low-valence I^-. UV-vis and Raman spectroscopy were further employed to investigate the valence state evolution of iodine species at different charge/discharge stages (**Figure 3**b-d). As shown in Figure 3c, an adsorption peak shows up at 465 nm at the early charge stage. It corresponds to I_2 and suggests the I^-/I^0 conversion. Further charging the cathode generates another adsorption peak at around 360 nm, which is assigned to the formation of I^+ from the I^0/I^+ reaction. Raman spectra at various charge/discharge states reveal similar results. Characteristic peaks corresponding to the I^+-urea complex emerged at ~165 cm^{-1} when charged at high voltage and vanished during discharge (**Figure 3**d).[33,34] The above characterizations offer solid evidence that urea can activate the I^0/I^+ conversion in zinc-iodine cells, and the reaction is highly reversible.

CV measurements were carried out at different scan rates ranging from 0.2 to 1.0 mV s^{-1} to better understand the conversion reaction kinetics of the PVPI cathode in the $Zn(OTf)_2$/urea system. As shown in **Figure 3**e, the two pairs of redox peaks correspond to the I^+/I^0 and I^0/I^- conversion reactions, respectively. The correlation between the peak current (i) and scan rate (v) can be described by the formula: $i = av^b$, where a and b are two constants. The linear fittings in **Figure 3**f determine the b values for four peaks to be 0.70, 0.62, 0.67, and 0.61, respectively, which suggests combined diffusion-controlled (b = 0.5) and non-diffusion-controlled (b = 1) charge storage processes. The contribution from two processes can be separated based on the equation: $i = k_1v + k_2v^{1/2}$, where k_1 and k_2 are two constants, and k_1v and $k_2v^{1/2}$ correspond to non-diffusion-controlled

and diffusion-controlled charge storage capacities, respectively. As summarized in **Figure 3**g, the non-diffusion-controlled process contributes 42% of the overall specific capacity at a scan rate of 0.2 mV s^{-1}, gradually increasing to 61% at 1.0 mV s^{-1}. The reaction kinetics of $I^-/I^0/I^+$ conversion in the $Zn(OTf)_2$/urea system were further studied based on the Tafel slope (η) obtained from CV curves (**Figure 3**h). As plotted in **Figure S5**, the I^+/I^0 conversion reaction exhibits smaller Tafel slopes (80 and 88 mV dec^{-1}) than I^-/I^0 (129 and 175 mV dec^{-1}), implying its faster conversion kinetics.[42] Meanwhile, the ion diffusion coefficients over the charge/discharge process have been determined by the galvanostatic intermittent titration technique (GITT) test (**Figure 3**i,j). The diffusion coefficients at lower working potentials are generally smaller than those at higher potentials, which benefits more rapid kinetics of the I^0/I^+ conversion reaction.

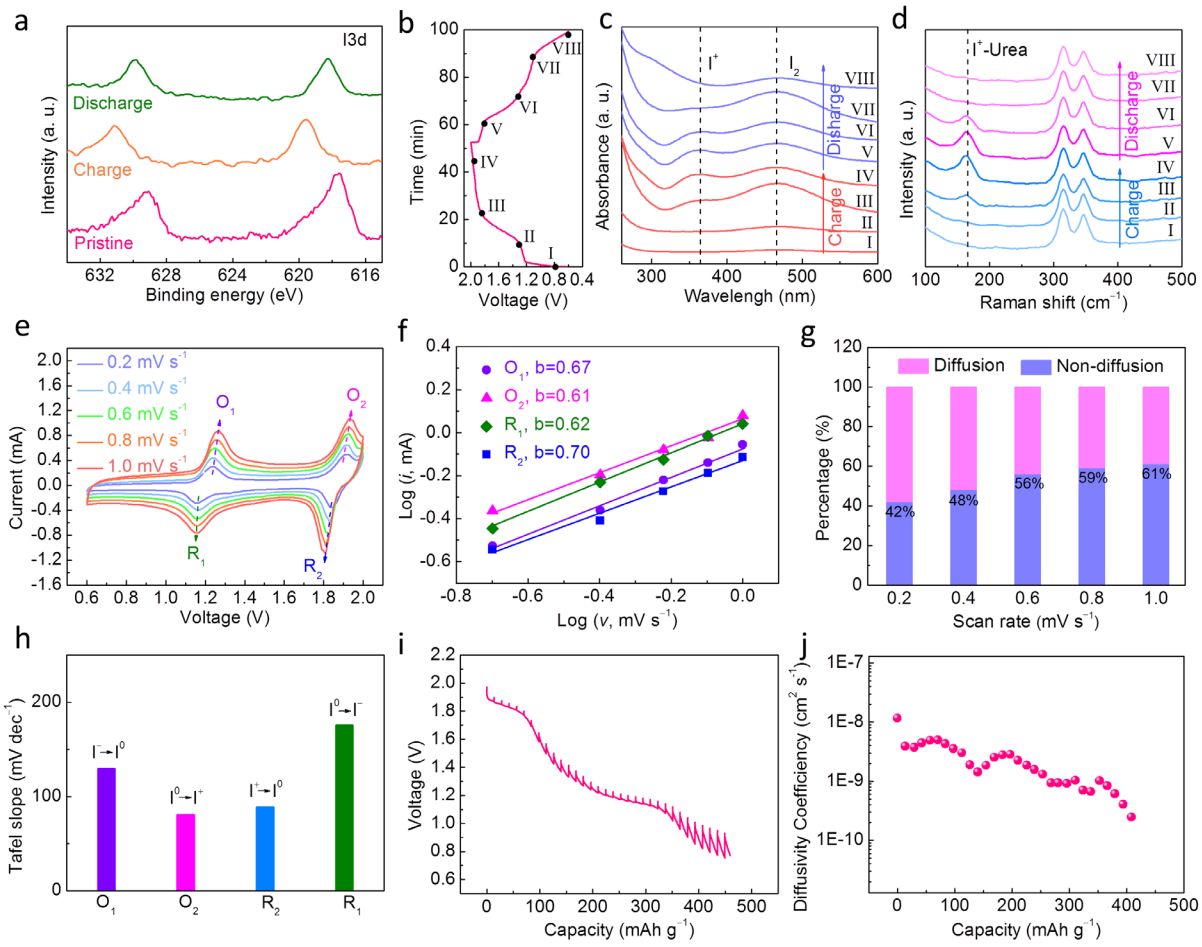

Figure 3. a) I3d XPS spectra of the pristine, fully charged, and fully discharged PVPI cathode. b) Charge-discharge curve. c) UV-vis spectra and d) Raman spectra at different charge/discharge states. e) CV curves of the PVPI cathode at different scan rates. f) The linear fits of log(*i*) vs. log(*v*) plots. g) Non-diffusion-controlled capacity contributions at different scan rates. h) The conversion kinetics analysis of I_2. i) GITT curves of the PVPI cathode. j) The diffusion coefficient is calculated from the GITT curve.

To assess the feasibility of real-world applications, Zn//PVPI pouch cells were fabricated with the $Zn(OTf)_2$/urea electrolyte. The configuration and optical image of the as-fabricated pouch cell are illustrated in **Figure 4**a. The resulting charge/discharge curve is plotted in **Figure S6**, showing

the maintaining of the high voltage plateau at 1.8 V. The mechanical stability was attested using the bending/cutting test. As demonstrated in **Figure 4**b, the electronic clock could be powered by the pouch cell even after bending at different angles or cutting, revealing its excellent flexibility and practical feasibility. The long-term cycling test demonstrates an initial reversible capacity of 219 mAh g^{-1}, slightly decreasing to 200 mAh g^{-1} after prolonged 700 charge/discharge cycles (**Figure 4**c). The results confirm the outstanding cycling performance of our zinc-iodine system.

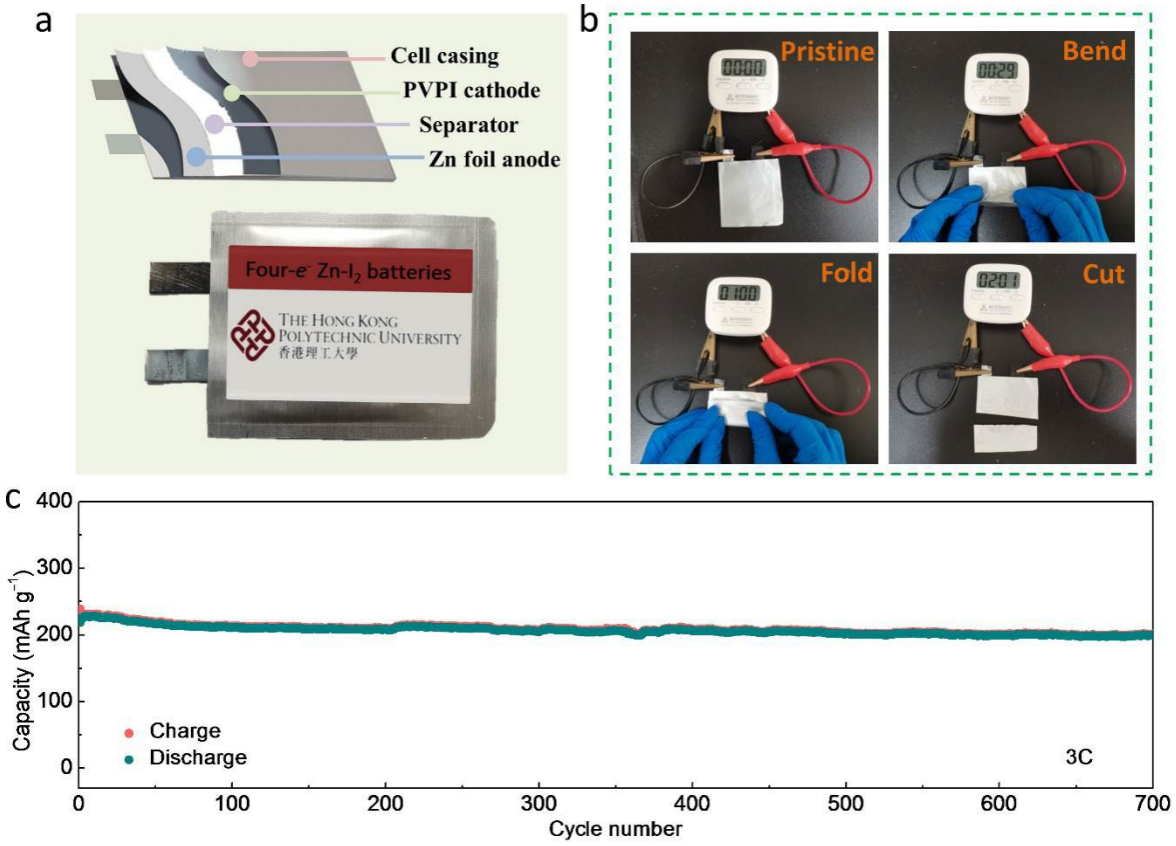

Figure 4. a) The schematic illustration of the Zn||PVPI pouch cell configuration. b) The Zn//PVPI pouch cell drove an electronic clock after bending at different angles and cutting. c) Cycling performance of Zn//PVPI pouch cell at 3C.

CONCLUSION

In summary, we have developed a halogen-free and cost-effective aqueous electrolyte to realize stable $I^-/I^0/I^+$ conversion electrochemistry in zinc-iodine batteries. A urea additive in the $Zn(OTf)_2$ aqueous electrolyte activates the I^0/I^+ redox couple and stabilizes I+, which enables a record-high plateau voltage of 1.8 V vs. Zn/Zn^{2+}. DFT calculations combining spectroscopy studies and electrochemical kinetics analyses demonstrate more thermodynamically favorable for I^0/I^+ conversion and inhibited self-disproportionation of I^+ by coordinating electron-deficient I^+ with electron-rich oxygen and nitrogen sites on urea to form a chelation structure, thus promoting rapid kinetics and excellent reversibility. Moreover, urea reduces the H_2O activity of the electrolyte by hydrogen bonds to further inhibit the hydrolysis of I^+. As a result, the as-fabricated Zinc-iodine battery delivers high specific capacities of 419 mAh g^{-1} at 1C and 285 mAh g^{-1} at 5C. It also exhibits excellent cycling stability with 147 mAh g^{-1} capacity maintained after prolonged 10000 cycles. This study thus provides a new approach for achieving high-voltage redox chemistry in aqueous zinc-iodine batteries.

EXPERIMENTAL SECTION

Materials: The chemicals in this work were all commercially available and used as received. Zinc foil (99.9%, thickness of 0.15–0.25 mm), zinc chloride ($ZnCl_2$, >99.0%), and sodium alginate were purchased from Sinopharm Chemical Reagent Co., Ltd. Glass fiber (GF/A) was purchased from Whatman. Zinc trifluoromethane sulfonate ($Zn(OTf)_2$, >98.0%), polyvinylpyrrolidone-iodine (PVPI), and urea (>99.0%) were purchased from Aladdin (Shanghai, China).

Material characterization: Fourier transform infrared spectroscopy (FTIR) was conducted by a Bruker INVENIO S. The UV-vis spectra were collected in a Lambda XLS+UV-vis spectrometer. The X-ray photoelectron spectroscopy (XPS) spectra were measured on a Thermo Scientific

spectrometer with an Al-Kα X-ray source. The data was analyzed with CasaXPS software by calibrating the C 1s peak to 284.8 eV. Raman spectra were collected on HORIBA (JOBIIN YVON French) Raman spectrum analyzer using a 532 nm laser. 1H NMR was performed on Bruker AVANCE 400MHz.

Electrochemical measurements: The active material of PVPI, conductive additive of ketjen black (KB), and binder of sodium alginate were mixed at a mass ratio of 7:2:1 and dispersed in water to make a slurry. Then, the slurry was coated onto a carbon paper substrate and dried at room temperature. The iodine loading was controlled to be 0.8–1.0 mg cm^{-2}. CR2032 coin cells were assembled in an ambient atmosphere comprising Zn foil anode, 4 m $Zn(OTf)_2$, 4 m $ZnCl_2$, or 4 m $Zn(OTf)_2$+6 m urea electrolyte, glass fiber separator, and PVPI cathode. All applied current rates, and specific capacities were based on the mass of the active iodine. The pouch cell was assembled with the PVPI cathode size of 4×4 cm^2, the glass fiber separator size of 5×5 cm_2, and the Zn foil anode size of 4×4 cm^2. Galvanostatic charge/discharge and CV tests were performed on a battery tester (CT2001A, LAND, China) and electrochemical workstation (Bio-Logic, VMP3) in the voltage range of 0.6−2.0 V vs. Zn2+/Zn, respectively. The ion diffusion coefficient (D) was calculated from GITT based on the following formula:[9]

$$D = \frac{4L^2}{\pi\tau}\left(\frac{\Delta E_S}{\Delta E_t}\right)^2$$

Here, τ was the relaxation time, ΔE_S was the steady-state potential change after a single pulse, and ΔE_t was the potential change during a pulse after eliminating the IR drop. The diffusion length L was measured by the geometric thickness of the cathode.

Computational methods: DFT calculations were performed using Gaussian 16.[43] All structures were optimized by using B3LYP functional with the LANL2DZ basis set.[44] All calculations were carried out with atom-pairwise dispersion correction (DFT-D3) and the implicit universal solvation model was based on the solute electron density (SMD).[45]

The binding energies between I^+ and various organic molecules were calculated by the following equation:[46]

$$E_b = E_{molecules+I+} - E_{molecules} - E_{I+}$$

where E_b was the binding energy between I^+ and the organic molecule, and $E_{molecules+I+}$, $E_{molecules}$, and E_{I+} were the energies of the I^+-organic molecule complex, the organic molecule, and I^+, respectively.

ASSOCIATED CONTENT

Supporting Information

Supporting Information is available free of charge on the ACS Publications website or from the author.

AUTHOR INFORMATION

Corresponding Author

Xiaoliang Yu−Department of Mechanical Engineering and Research Institute for Smart Energy, The Hong Kong Polytechnic University, Hong Kong 999077, China; E-mail: xiaoliang.yu@polyu.edu.hk

Guohua Chen−School of Energy and Environment, City University of Hong Kong, Hong Kong 999077, China; E-mail: guohchen@cityu.edu.hk

Xiaoqi Sun−Department of Chemistry, Northeastern University, Shenyang 110819, China; E-mail: sunxiaoqi@mail.neu.edu.cn.

Notes

The authors declare no competing financial interests.

ACKNOWLEDGMENT

This work was supported by the Natural Science Foundation of Guangdong (No. 2023A1515010020) and National Nature Science Foundation of China (52402052, 52174276).

REFERENCES

(1) Ruan, P.; Liang, S.; Lu, B.; Fan, H. J.; Zhou, J., Design Strategies for High-Energy-Density Aqueous Zinc Batteries. *Angew. Chem. Int. Ed.* **2022**, 61, 1-15.

(2) Wang, X.; Zhang, Z.; Xi, B.; Chen, W.; Jia, Y.; Feng, J.; Xiong, S., Advances and Perspectives of Cathode Storage Chemistry in Aqueous Zn-Ion Batteries. *ACS Nano* **2021**, 15, 9244-9272.

(3) Sun, W.; Wang, F.; Zhang, B.; Zhang, M.; Küpers, V.; Ji, X.; Theile, C.; Bieker, P.; Xu, K.; Wang, C.; Winter, M., A rechargeable zinc-air battery based on zinc peroxide chemistry. *Science* **2021**, 371, 46-51.

(4) Liu, Y.; Wang, K.; Yang, X.; Liu, J.; Liu, X.-X.; Sun, X., Contribution in MnO_2 Cathode Material by Structural Engineering for Stable Cycling in Aqueous Zn Batteries. *ACS Nano* **2023**, 17, 14792-14799.

(5) Zampardi, G.; La Mantia, F., Open challenges and good experimental practices in the research field of aqueous Zn-ion batteries. *Nat. Commun.* **2022**, 13, 687.

(6) Liu, H.; Jiang, L.; Cao, B.; Du, H.; Lu, H.; Ma, Y.; Wang, H.; Guo, H.; Huang, Q.; Xu, B.; Guo, S., Van der Waals Interaction-Driven Self-Assembly of V_2O_5 Nanoplates and MXene for High-Performing Zinc-Ion Btteries by Suppessing Vanadium Dissolution. *ACS Nano* **2022**, 16, 14539-14548.

(7) Zhu, K.; Wu, T.; Bergh, W.; Stefik, M.; Huang, K., Reversible Molecular and Ionic Storage Mechanisms in High-Performance $Zn_{0.1}V_2O_5 \cdot nH_2O$ Xerogel Cathode for Aqueous Zn-Ion Batteries. *ACS Nano* **2021**, 15, 10678-10688.

(8) Sun, W.; Wang, F.; Hou, S.; Yang, C.; Fan, X.; Ma, Z.; Gao, T.; Han, F.; Hu, R.; Zhu, M.; Wang, C., Zn/MnO_2 Battery Chemistry With H^+ and Zn^{2+} Coinsertion. *J. Am. Chem. Soc.* **2017**, 139, 9775-9778.

(9) Lin, Z.; Shi, H. Y.; Lin, L.; Yang, X.; Wu, W.; Sun, X., A high capacity small molecule quinone cathode for rechargeable aqueous zinc-organic batteries. *Nat. Commun.* **2021**, 12, 4424.

(10) Lin, L.; Lin, Z.; Zhu, J.; Wang, K.; Wu, W.; Qiu, T.; Sun, X., A semi-conductive organic cathode material enabled by extended conjugation for rechargeable aqueous zinc batteries. *Energy Environ. Sci.* **2023**, 16, 89-96.

(11) Sun, T.; Yi, Z.; Zhang, W.; Nian, Q.; Fan, H. J.; Tao, Z., Dynamic Balance of Partial Charge for Small Organic Compound in Aqueous Zinc-Organic Battery. *Adv. Funct. Mater.* **2023**, 33, 2306675.

(12) Wu, W.; Wang, S.; Lin, L.; Shi, H.-Y.; Sun, X., A dual-mediator for a sulfur cathode approaching theoretical capacity with low overpotential in aqueous Zn–S batteries. *Energy Environ. Sci.* **2023**, 16, 4326-4333.

(13) Hao, J.; Zhang, S.; Wu, H.; Yuan, L.; Davey, K.; Qiao, S.-Z., Advanced cathodes for aqueous Zn batteries beyond Zn^{2+} intercalation. *Chem. Soc. Rev.* **2024**, 53, 4312-4332.

(14) Gao, W.; Cheng, S.; Zhang, Y.; Xie, E.; Fu, J., Efficient Charge Storage in Zinc – Iodine Batteries based on Pre-Embedded Iodine-Ions with Reduced Electrochemical Reaction Barrier and Suppression of Polyiodide Self-Shuttle Effect. *Adv. Funct. Mater*. **2023**, 33, 2211979.

(15) Hu, X.; Zhao, Z.; Yang, Y.; Zhang, H.; Lai, G.; Lu, B.; Zhou, P.; Chen, L.; Zhou, J., Bifunctional self-segregated electrolyte realizing high-performance zinc-iodine batteries. InfoMat *2024*, e12620.

(16) Zhang, L.; Guo, H.; Zong, W.; Huang, Y.; Huang, J.; He, G.; Liu, T.; Hofkens, J.; Lai, F., Metal–iodine batteries: achievements, challenges, and future. *Energy Environ. Sci.* **2023**, 16, 4872-4925.

(17) Chen, H.; Li, X.; Fang, K.; Wang, H.; Ning, J.; Hu, Y., Aqueous Zinc-Iodine Batteries: From Electrochemistry to Energy Storage Mechanism. *Adv. Energy Mater.* **2023**, 13, 2302187.

(18) Li, X.; Li, M.; Huang, Z.; Liang, G.; Chen, Z.; Yang, Q.; Huang, Q.; Zhi, C., Activating the I^0/I^+ redox couple in an aqueous I_2–Zn battery to achieve a high voltage plateau. *Energy Environ. Sci.* **2021**, 14, 407-413.

(19) Zou, Y.; Liu, T.; Du, Q.; Li, Y.; Yi, H.; Zhou, X.; Li, Z.; Gao, L.; Zhang, L.; Liang, X., A four-electron Zn-I_2 aqueous battery enabled by reversible $I^-/I_2/I^+$ conversion. *Nat. Commun.* **2021**, 12, 170.

(20) Y. L. Wang, J. C. N. a. D. W. M., kinetics of hydrolysis of iodine monochloride measured by the pulsed-accelerated-flow method. *J. Am. Chem. Soc.* **1989**, 111, 7838–7844.

(21) Philbrick, F. A., the hydrolysis of iodine monochloride. *J. Am. Chem. Soc.* **1934**, 56, 1257–1259.

(22) Liu, T.; Lei, C.; Wang, H.; Li, J.; Jiang, P.; He, X.; Liang, X., Aqueous Electrolyte With Weak Hydrogen Bonds for Four-Electron Zinc-Iodine Battery Operates in a Wide Temperature Range. *Adv. Mater.* **2024**, 36, 2405473.

(23) Lv, S.; Fang, T.; Ding, Z.; Wang, Y.; Jiang, H.; Wei, C.; Zhou, D.; Tang, X.; Liu, X., A High-Performance Quasi-Solid-State Aqueous Zinc–Dual Halogen Battery. *ACS Nano* **2022**, 16, 20389-20399.

(24) Liu, T.; Lei, C.; Wang, H.; Xu, C.; Ma, W.; He, X.; Liang, X., Practical four-electron zinc-iodine aqueous batteries enabled by orbital hybridization induced adsorption-catalysis. *Sci. Bulletin* **2024**, 69, 1674-1685.

(25) Wang, C.; Ji, X.; Liang, J.; Zhao, S.; Zhang, X.; Qu, G.; Shao, W.; Li, C.; Zhao, G.; Xu, X.; Li, H., Activating and stabilizing a reversible four electron redox reactions of I^-/I^+ for aqueous Zn‐iodine battery. *Angew. Chem. Int. Ed.* **2024**, 63, e202403187.

(26) Zong, W.; Li, J.; Zhang, C.; Dai, Y.; Ouyang, Y.; Zhang, L.; Li, J.; Zhang, W.; Chen, R.; Dong, H.; Gao, X.; Zhu, J.; Parkin, I. P.; Shearing, P. R.; Lai, F.; Amine, K.; Liu, T.; He, G., Dynamical Janus Interface Design for Reversible and Fast-Charging Zinc–Iodine Battery under Extreme Operating Conditions. *J. Am. Chem. Soc.* **2024**, 146, 21377-21388.

(27) Turunen, L.; Erdélyi, M., Halogen bonds of halonium ions. *Chem. Soc. Rev.* **2020**, 49, 2688-2700.

(28) Li, W.; Xu, H.; Zhang, H.; Wei, F.; Zhang, T.; Wu, Y.; Huang, L.; Fu, J.; Jing, C.; Cheng, J.; Liu, S., Designing Ternary Hydrated Eutectic Electrolyte Capable of Four-Electron Conversion for Advanced Zn-I_2 Full Batteries. *Energy Environ. Sci.* **2023**, 16, 4502-4510.

(29) Zhang, S.; Tan, X.; Meng, Z.; Tian, H.; Xu, F.; Han, W.-Q., Naturally abundant high-performance rechargeable aluminum/iodine batteries based on conversion reaction chemistry. *J. Mater. Chem. A* **2018**, 6, 9984-9996.

(30) Yu, S.; Kumar, P.; Ward, J. S.; Frontera, A.; Rissanen, K., A "nucleophilic" iodine in a halogen-bonded iodonium complex manifests an unprecedented $I^{+}\cdots Ag^{+}$ interaction. *Chem* **2021**, 7, 948-958.

(31) Zhang, C.; Holoubek, J.; Wu, X.; Daniyar, A.; Zhu, L.; Chen, C.; Leonard, D. P.; Rodríguez-Pérez, I. A.; Jiang, J.-X.; Fang, C.; Ji, X., A $ZnCl_2$ water-in-salt electrolyte for a reversible Zn metal anode. *Chem. Commun.* **2018**, 54, 14097-14099.

(32) Kang, J.; Wang, C.; Liu, Z.; Wang, L.; Meng, Y.; Zhai, Z.; Zhang, J.; Lu, H., Electron-outflowing heterostructure hosts for high-voltage aqueous zinc-iodine batteries. *Energy Storage Mater.* **2024**, 68, 103367.

(33) Jiang, P.; Du, Q.; Lei, C.; Xu, C.; Liu, T.; He, X.; Liang, X., Stabilized four-electron aqueous zinc–iodine batteries by quaternary ammonium complexation. *Chem. Sci.* **2024**, 15, 3357-3364.

(34) Wang, M.; Meng, Y.; Sajid, M.; Xie, Z.; Tong, P.; Ma, Z.; Zhang, K.; Shen, D.; Luo, R.; Song, L.; Wu, L.; Zheng, X.; Li, X.; Chen, W., Bidentate Coordination Structure Facilitates High-Voltage and High-Utilization Aqueous Zn-I_2 Batteries. *Angew. Chem. Int. Ed.* **2024**, 63, e202404784.

(35) Cui, H.; Wang, T.; Huang, Z.; Liang, G.; Chen, Z.; Chen, A.; Wang, D.; Yang, Q.; Hong, H.; Fan, J.; Zhi, C., High-Voltage Organic Cathodes for Zinc-Ion Batteries through Electron Cloud and Solvation Structure Regulation. *Angew. Chem. Int. Ed.* **2022**, 61, e202203453.

(36) Keuleers, R.; Desseyn, H. O.; Rousseau, B.; Alsenoy, C. V., Vibrational Analysis of Urea. *J. Phys. Chem. A* **1999**, 103, 4621–4630.

(37) Wang, Z.; Diao, J.; Burrow, J. N.; Reimund, K. K.; Katyal, N.; Henkelman, G.; Mullins, C. B., Urea-Modified Ternary Aqueous Electrolyte With Tuned Intermolecular Interactions and Confined Water Activity for High-Stability and High-Voltage Zinc-Ion Batteries. *Adv. Funct. Mater.* **2023**, 33, 2304791.

(38) Xu, J.; Ji, X.; Zhang, J.; Yang, C.; Wang, P.; Liu, S.; Ludwig, K.; Chen, F.; Kofinas, P.; Wang, C., Aqueous Electrolyte Design for Super-Stable 2.5 V $LiMn_2O_4$|| $Li_4Ti_5O_{12}$ Pouch Cells. *Nat. Energy* **2022**, 7, 186-193.

(39) Finer, E. G.; Franks, F.; Tait, M. J., Nuclear Magnetic Resonance Studies of Aqueous Urea Solutions. *J. Am. Chem. Soc.* **1972**, 94, 4424–4429.

(40) Xie, J.; Liang, Z.; Lu, Y.-C., Molecular crowding electrolytes for high-voltage aqueous batteries. Nature materials 2020, 19, 1006-1011.

(41) Lukatskaya, M. R.; Feldblyum, J. I.; Mackanic, D. G.; Lissel, F.; Michels, D. L.; Cui, Y.; Bao, Z., Concentrated Mixed Cation Acetate "Water-in-Salt" Solutions as Green and Low-Cost High Voltage Electrolytes for Aqueous Batteries. *Energy Environ. Sci.* **2018**, 11, 2876-2883.

(42) Ma, L.; Ying, Y.; Chen, S.; Huang, Z.; Li, X.; Huang, H.; Zhi, C., Electrocatalytic Iodine Reduction Reaction Enabled by Aqueous Zinc-Iodine Battery with Improved Power and Energy Densities. *Angew. Chem. Int. Ed.* **2021**, 60, 3791-3798.

(43) Adamo, C.; Scuseria, G. E.; Barone, V., Accurate Excitation Energies from Time-Dependent Density Functional Theory: Assessing the PBE0 Model. *J. Chem. Phys.* **1999**, 111, 2889-2899.

(44) Zhang, Z.; Zhu, Y.; Yu, M.; Jiao, Y.; Huang, Y., Development of Long Lifespan High-Energy Aqueous Organic||Iodine Rechargeable Batteries. *Nat. Commun.* **2022**, 13, 6489.

(45) Zhu, J.; Ji, P., Dispersion Relation and Landau Damping of Waves in High-Energy Density Plasmas. *Plasma Phys. Control. Fusion* **2012**, 54, 065004.

(46) Li, C.; Hu, L.; Ren, X.; Lin, L.; Zhan, C.; Weng, Q.; Sun, X.; Yu, X., Asymmetric Charge Distribution of Active Centers in Small Molecule Quinone Cathode Boosts High-Energy and High-Rate Aqueous Zinc-Organic Batteries. *Adv. Funct. Mater.* **2024**, 34, 2313241.

Table of Contents

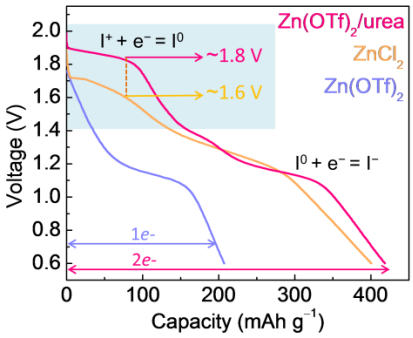

We have developed a halogen-free electrolyte to realize stable $I^-/I^0/I^+$ conversion in aqueous zinc-iodine batteries. The coordination between electron-deficient I+ and electron-rich ON (urea) is more thermodynamically favorable for I^0/I^+ conversion and inhibits the self-disproportionation of I^+, which promotes rapid kinetics and excellent reversibility. As a result, a record-high plateau voltage of 1.8 V vs. Zn/Zn^{2+} is achieved.